ANL/ET/CP--80144
Conf-931079--17

IRRADIATION-ASSISTED STRESS CORROSION CRACKING OF MATERIALS FROM COMMERCIAL BWRs: ROLE OF GRAIN-BOUNDARY MICROCHEMISTRY*

by

H. M. Chung, W. E. Ruther, J. E. Sanecki, A. G. Hins, and T. F. Kassner

Energy Technology Division
Argonne National Laboratory
Argonne, IL 60439

December 1993

DISCLAIMER

To be published in the Proceedings of the 21st Water Reactor Safety Information Meeting, October 25-28, 1993, Bethesda, MD

*Work supported by the Office of Nuclear Regulatory Research, U. S. Nuclear Regulatory Commission

IRRADIATION-ASSISTED STRESS CORROSION CRACKING OF MATERIALS FROM COMMERCIAL BWRs: ROLE OF GRAIN-BOUNDARY MICROCHEMISTRY*

H. M. Chung, W. E. Ruther, J. E. Sanecki, A. G. Hins, and T. F. Kassner

Energy Technology Division
Argonne National Laboratory
Argonne, IL 60439

ABSTRACT

Constant-extension-rate tensile tests and grain-boundary analysis by Auger electron spectroscopy were conducted on high- and commercial-purity (HP and CP) Type 304 stainless steel (SS) specimens from irradiated boiling-water reactor (BWR) components to determine susceptibility to irradiation-assisted stress corrosion cracking (IASCC) and to identify the mechanisms of intergranular failure. The susceptibility of HP neutron absorber tubes to intergranular stress corrosion cracking (IGSCC) was higher than that of CP absorber tubes or CP control blade sheath. Contrary to previous beliefs, susceptibility to intergranular fracture could not be correlated with radiation-induced segregation of impurities such as Si, P, C, N, or S, but a correlation was obtained with grain-boundary Cr concentration, indicating a role for Cr depletion that promotes IASCC. Detailed analysis of grain-boundary chemistry was conducted on neutron absorber tubes that were fabricated from two similar heats of HP Type 304 SS of virtually identical bulk chemical composition but exhibiting a significant difference in susceptibility to IGSCC for similar fluence. Grain-boundary concentrations of Cr, Ni, Si, P, S, and C in the crack-resistant and -susceptible HP heats were virtually identical. However, grain boundaries of the cracking-resistant material contained less N and more B and Li (transmutation product from B) than those of the crack-susceptible material, indicating beneficial effects of low N and high B contents.

INTRODUCTION

In recent years, failures of nonsensitized austenitic stainless steel (SS) core internal components in both boiling- and pressurized-water reactors (BWRs and PWRs) have increased after accumulation of relatively high fluence (>5 x 10^{20} n cm^{-2}, E >1 MeV). Although most failed components can be replaced, some safety-significant structural components, such as the BWR top guide, shroud, and core plate, would be very difficult or impractical to replace. Therefore, the structural integrity of these components after accumulation of high fluence has been a subject of concern, and extensive research has been conducted to provide an understanding of this type of degradation, which is commonly known as irradiation-assisted stress corrosion cracking (IASCC).

IASCC failures have been attributed to radiation-induced segregation (RIS) or depletion of impurity and alloying elements at grain boundaries. As early as in the mid-1960s, investigators began to implicate impurities such as Si, P, and S in IASCC failure of fuel cladding fabricated from solution-annealed nonsensitized austenitic stainless steel.[1-5] Since then, it seemed that the concept of superior resistance of high-purity (HP) materials of SSs low in Si, P, S, and C was proved valid after favorable experience with HP Type 348 SS fuel cladding in the La Crosse boiling-water reactor (BWR)[6] and the subsequent demonstration of superior performance of the low-N HP 348 SS heat from swelling-tube tests in a BWR and a pressurized-water reactor (PWR).[7-8] Although data were very limited, results from a laboratory constant-extension-rate tensile (CERT) test[9] also suggest superior performance of the same HP heat of Type 348 SS investigated by the authors of Refs. 6-8. The superior performance seemed to indicate that radiation-induced segregation (RIS) of Si is the predominant process, because RIS of other impurities and Cr depletion in the HP

---

* Work supported by the U.S. Nuclear Regulatory Commission, Office of Nuclear Regulatory Research.

and commercial-purity (CP) Type 348 SS were either similar or could not be detected by field-emission-gun scanning transmission electron microscopy (FEG-STEM).[9] It has also been reported that Type 316L SS, irradiated in the mixed-spectrum Advanced Test Reactor (ATR), exhibited better resistance to stress corrosion cracking (SCC) than Type 316NG SS,[10] indicating a possible benefit of low N.

On the basis of these experiences with Type 348 and 316 SS, HP materials of Type 304 SS have been suggested as a better alternative to CP Type 304 SS, a material from which the majority of core internal components of operating BWRs and PWRs in U.S. have been fabricated. Recently, Jacobs reported that neutron absorber tubes (QC-AT, Table 1) fabricated from one HP heat (HP304-CD, Table 1) of Type 304 SS performed better than similar counterparts fabricated from CP Type 304 SS in noncreviced positions in the BWR control blade.[11]

However, in direct contradiction of the above experiences, results from CERT tests conducted on other BWR neutron absorber tubes indicated that the resistance of other similar HP heats of Type 304 SS is worse than that of CP materials.[12-13] Results consistent with this have also been reported for Type 304 SS specimens irradiated by either neutrons,[14] ions,[15] or protons.[16] Therefore, the issue of superior performance of HP materials and the mechanisms of IASCC appear to be far from established. Nevertheless, one important point seems to be quite clear: heat-to-heat variation in susceptibility to IASCC can be very large, even among HP materials of virtually identical chemical composition. This seems to pose an important question not only about the role of grain-boundary segregation of other impurities (i.e., impurities other than Si, P, S, and C) but also about the premise that Cr depletion is the primary mechanism of IASCC.

To provide a better answer to this question, CERT tests were conducted on specimens obtained from neutron absorber tubes and a control blade sheath fabricated from several heats of HP- and CP-grade Type 304 SS and irradiated to high fluence during actual service in a BWR. Results from the CERT tests were correlated with results of microstructural analysis by Auger electron spectroscopy (AES) to identify the primary process that controls susceptibility to IGSCC and in-reactor performance of Type 304 SS components.

Among the several materials tested was a unique pair of BWR neutron absorber tubes fabricated from two HP heats of virtually identical chemical composition but exhibiting a significant difference in susceptibility to intergranular stress corrosion cracking (IGSCC) during CERT tests. One of the detailed analyses of grain-boundary microchemistry was conducted on neutron absorber tubes (QC-AT, Table 1), fabricated from the HP Heat HP304-CD, of which superior in-reactor performance has been reported by Jacobs.[11] The other analysis was conducted on neutron absorber tubes (V-AT), which were fabricated from a similar HP heat (HP304-A) of virtually identical chemical composition but one that exhibited a relatively high susceptibility to IGSCC during CERT tests.[12-13] CERT tests independent of those in Refs. 12 and 13 were conducted on both materials, and the result showed that IGSCC susceptibility of the former material (QC-AT) was significantly lower than that of the latter (V-AT) for a similar fluence level.[17] Chemical compositions of the IGSCC-resistant and the -susceptible materials were virtually identical except for N. Therefore, a comparative analysis of grain-boundary microchemistry of the two materials was considered ideal to shed light on the cause of the significant difference in susceptibility to IGSCC.

The objective of this study was twofold: (1) to determine the susceptibility of HP and CP Type 304 SS components to IASCC after actual service in a BWR, and (2) to identify the cause of the strong heat-to-heat variation, thereby providing a better understanding of the primary process of IASCC, which is essential if we are to establish a method to evaulate long-term performance of safety-significant core internal structures.

EXPERIMENTAL PROCEDURES

Specimen preparation, procedures for CERT tests, and a description of the hot-cell CERT apparatus were presented previously.[12,13] Cylindrical tensile specimens were

sectioned from top-, middle-, and bottom-axial positions of neutron-absorber-rod tubes fabricated from several CP and HP heats of Type 304 SS and irradiated in several BWRs. Boron-carbide absorber was removed with diamond-tip drills. Sheet tensile specimens, fabricated from BWR control blade sheaths, were also tested. CERT tests were conducted in air and in simulated BWR water at 289°C at a strain rate of 1.65×10^{-7} s^{-1}. The dissolved O concentration and conductivity of the simulated BWR water were ≈0.3 ppm and 0.12 $\mu S \cdot cm^{-1}$, respectively. Analysis of the fracture surfaces of CERT specimens was conducted by scanning electron microscopy (SEM) to determine the types of fracture surface morphology.

The fast neutron fluence and chemical composition of the HP and CP heats of Type 304 SS are given in Table 1. The chemical compositions of the three HP heats are similar except for N. Boron content could not be determined with an accuracy of <0.001 wt.%; however, Heat HP304-CD had a higher B content than did Heats HP304-A or -B.

Grain-boundary microchemistry was analyzed with a JEOL Model JAMP-10 scanning Auger microscope (SAM). Specimens charged with H were fractured at room temperature in the ultrahigh vacuum (≈7 to 20 x 10^{-7} Pa) of the SAM to reveal IG-fracture surfaces. Hydrogen was charged into notched AES specimens for 48 h at 60°C in a solution of 100-mg/l $NaAsO_2$ dissolved in 0.1-N H_2SO_4 at a current density of ≈500 mA/cm^2. Intergranular fracture of the H-charged specimens was observed in bands underneath the free surface of the fractured specimen. Average penetration depth of the more-or-less uniform IG-fracture band was measured in each specimen. A depth profile of Cr was obtained as a function of sputter distance beneath a selected region of IG fracture produced by CERT tests. Details of the procedure have been described elsewhere.[13]

Table 1. Chemical Composition and Fluence of HP and CP Type 304 SS BWR Components.

Heat ID No.	Composition (wt.%)									Source Code	Service Reactor	Fluence (10^{21} $n \cdot cm^{-2}$)
	Cr	Ni	Mn	C	N	B	Si	P	S			
HP304-A	18.50	9.45	1.53	0.018	0.100	<0.001	<0.03	0.005	0.003	V-AT[a]	BWR-B	0.2-1.4
HP304-B	18.30	9.75	1.32	0.015	0.080	<0.001	0.05	0.005	0.005	V-AT[a]	BWR-B	0.2-1.4
HP304-CD	18.58	9.44	1.22	0.017	0.037	0.001	0.02	0.002	0.003	V-AT[a]	BWR-B	0.2-1.4
HP304-CD	18.58	9.44	1.22	0.017	0.037	0.001	0.02	0.002	0.003	QC-AT[a]	BWR-QC	2.0
CP304-A	16.80	8.77	1.65	0.08[b]	0.052	-	1.55	0.045[b]	0.030[b]	BL-AT[c]	BWR-Y	0.2-2.0
CP304-B	18-20	8-10.5	2.00[b]	0.08[b]	-	-	1.00[b]	0.045[b]	0.030[b]	LC-S[d]	BWR-LC	0.5-2.6

[a]High-purity neutron absorber tubes, OD = 4.78 mm, wall thickness = 0.63 mm, composition before irradiation.
[b]Represents maximum value in the specification; actual value not measured.
[c]Commercial-purity absorber tubes, OD = 4.78 mm, wall thickness = 0.79 mm, composition after irradiation.
[d]Commercial-purity control blade sheath, thickness 1.22 mm, actual composition not measured.

RESULTS AND DISCUSSION

Tensile Properties

Results of tensile tests, CERT, and SEM analyses of the specimens from the HP and CP absorber tubes and control blade sheaths are summarized in Table 2. Figures 1 and 2 show the yield strength (YS) and ultimate tensile strength (UTS) versus fast-neutron fluence (E >1 MeV) of the CP and HP neutron absorber tubes and control blade sheath strained to failure in air (from Table 2). The figures contain similar data for CP-grade tensile specimens of Types 304, 304L, 316L, and 316NG SS irradiated in the ATR at 300°C and reported by Jacobs et al.[10] Both the yield and ultimate tensile strengths of the CP-grade

BWR sheath (Heat CP304-B, Table 1) and HP-grade absorber tube (Heat HP304-A) are significantly higher than those of the ATR-irradiated specimens or than those of the CP 304 SS neutron absorber for comparable fluence. It appears that irradiation-induced hardening of the two heats (CP304-B and HP304-A) is more pronounced than that of other materials in Fig. 1 for comparable fluence. The cause of the significant heat-to-heat variation is not understood at present. The irradiation-induced hardening tends to reach saturation at fluence $\geq 2.5 \times 10^{21}$ n cm^{-2} (E > 1 MeV), or ≥3.6 dpa.

Figure 3 shows total elongation versus fast-neutron fluence for the HP and CP 304 SS neutron absorber tubes and control blade sheath. For comparison, similar data from Ref. 10 for CP heats of Type 304, 304L, 316L, and 316NG SS irradiated in the ATR at 300°C are also shown in the figure. The latter data were obtained at a significantly higher strain rate than that used in the present tensile tests, i.e., 4×10^{-4} s^{-1} versus 1.7×10^{-7} s^{-1}. Ductility appears to reach an asymptotic minimum value of ≈5% at fluence levels $>1.5 \times 10^{21}$ n·cm^{-2}. Total elongations of the BWR-irradiated materials are, however, considerably smaller than those of the ATR-irradiated materials at the high fluence level, i.e, 5-10 vs. 8-22%. Therefore, the higher tensile ductility and the lower strength associated with the test-reactor-irradiated specimens should be used with caution.

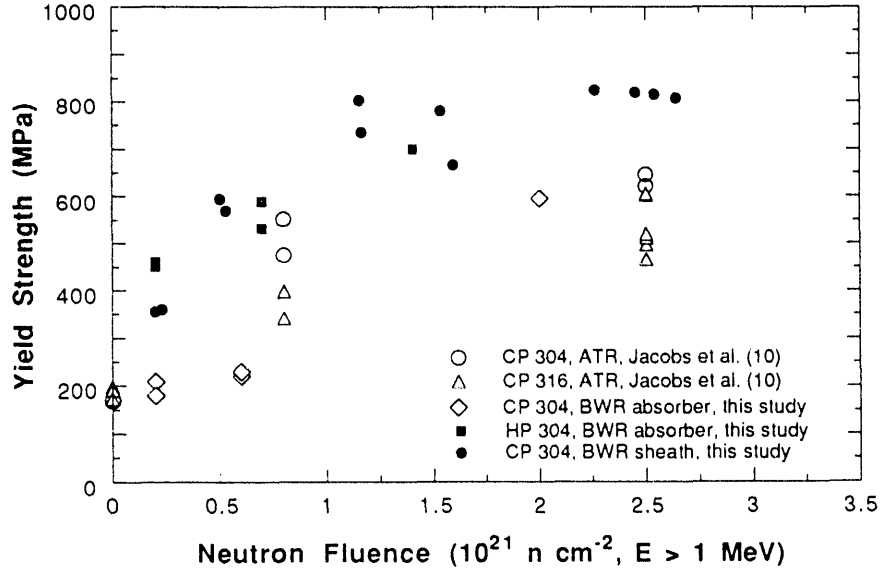

Figure 1. Yield stress vs. fast neutron fluence (E >1 MeV) for solution-annealed CP and HP Type 304 and 316 SS from tensile tests in air at 289°C.

Relative Susceptibilities of HP and CP Materials to IGSCC

The percent IGSCC measured in the BWR specimens has been plotted as a function of fast neutron fluence and yield strength in Figs. 4A and 4B, respectively. Similar results reported by Jacobs et al.[10,18] and Kodama et al.[19] are also shown in the figures. All data in Fig. 4A were obtained from BWR components at a comparable strain rate of $\approx 2 \times 10^{-7}$ s^{-1} in water containing ≈0.3 ppm dissolved O. The figure indicates that the IGSCC susceptibility of the CP control blade sheath is significantly lower than that of the CP neutron absorber

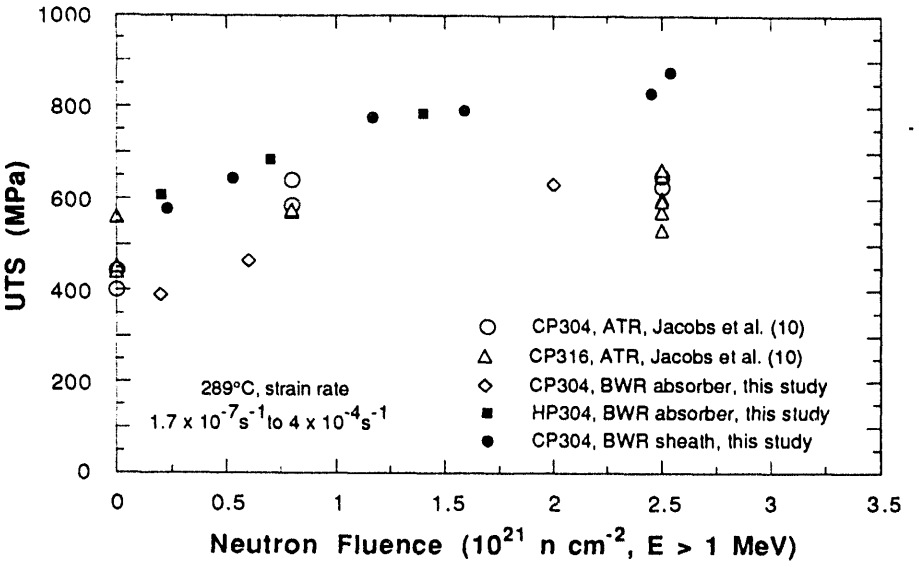

Figure 2. Ultimate tensile stress (UTS) vs. neutron fluence (E >1 MeV) for CP and HP Type 304 and 316 SS from tensile tests in air at 289°C

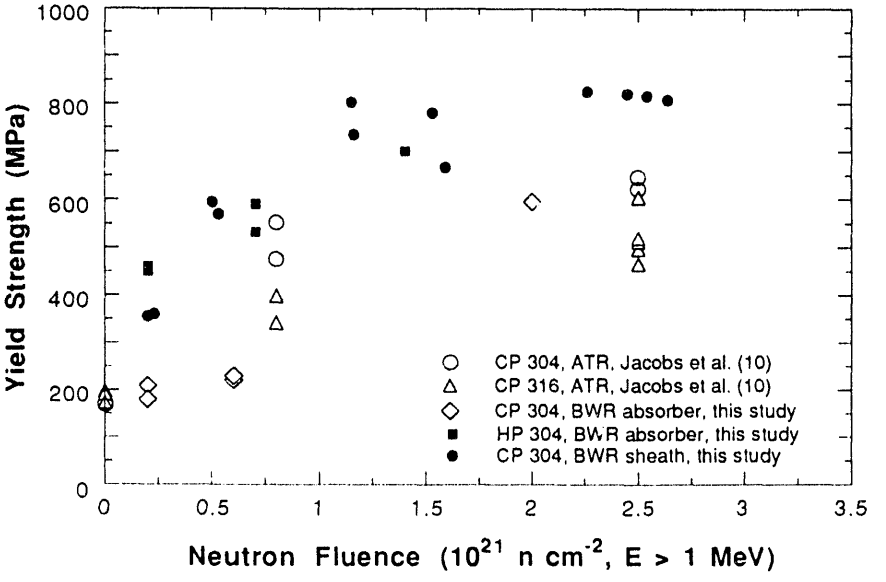

Figure 3. Total elongation vs. neutron fluence (E >1 MeV) for CP and HP Type 304 and 316 SS from tensile tests in air at 289°C

tube or the dry tube of Kodama et al.[19] for a comparable fluence level. The susceptibility of the HP absorber tube is greater than that of any of the CP materials.

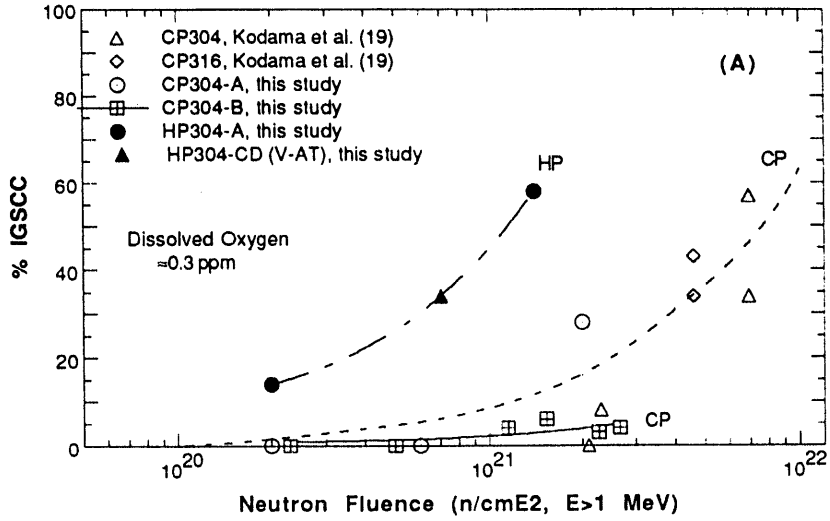

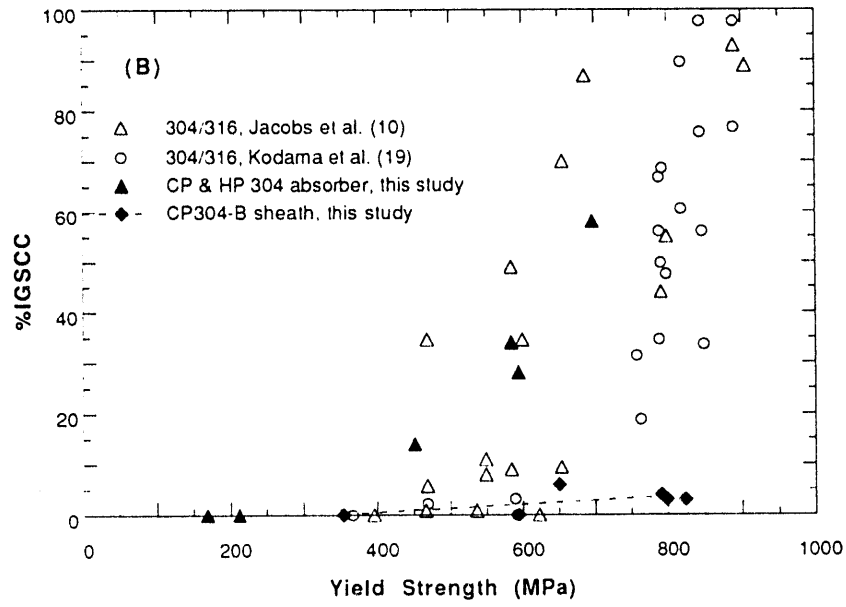

Fig. 4. Percent IGSCC vs. fluence (A) and vs. yield strength (B) for HP and CP Type 304 SS and CP 316 SS BWR components from CERT tests at 289°C in simulated BWR water.

Role of Irradiation Hardening

Figure 4B indicates that, apparently, no good correlation is observed between percent IGSCC and yield strength. For example, CP 304 SS sheath from the BWR-LC exhibited excellent resistance to IG cracking despite more pronounced irradiation-induced hardening for comparable fluence. For a similar yield strength of ≈800 MPa, percent IGSCC could be as high as 100% or as low as ≈3%, depending on composition and structure.

The rationale for implicating yield strength is that IASCC may be controlled primarily by irradiation hardening of grains regardless of a grain-boundary process that promotes stress corrosion. However, results given in Fig. 4B indicate clearly that, although irradiation-induced hardening is one of the necessary conditions of IASCC, which renders plastic deformation within grains more difficult, a certain grain-boundary process is essential to induce IGSCC in the irradiated materials in water.

Effects of Si, P, and S

Auger signals from several spots on ductile and intergranular fracture regions were analyzed, and peak-to-peak amplitudes of the primary peaks of Ni, Si, P, C, N, S, and the unidentified peak at ≈58-59 eV ($X_{59\text{-eV}}$) were measured and normalized with respect to the amplitude of the primary peak of Fe. These basic data from AES analyses were reported elsewhere.[12,13] From the data, degree of grain-boundary segregation of each element was determined. In Figs. 5A-5C, percent IGSCC from CERT tests in water has been plotted as a

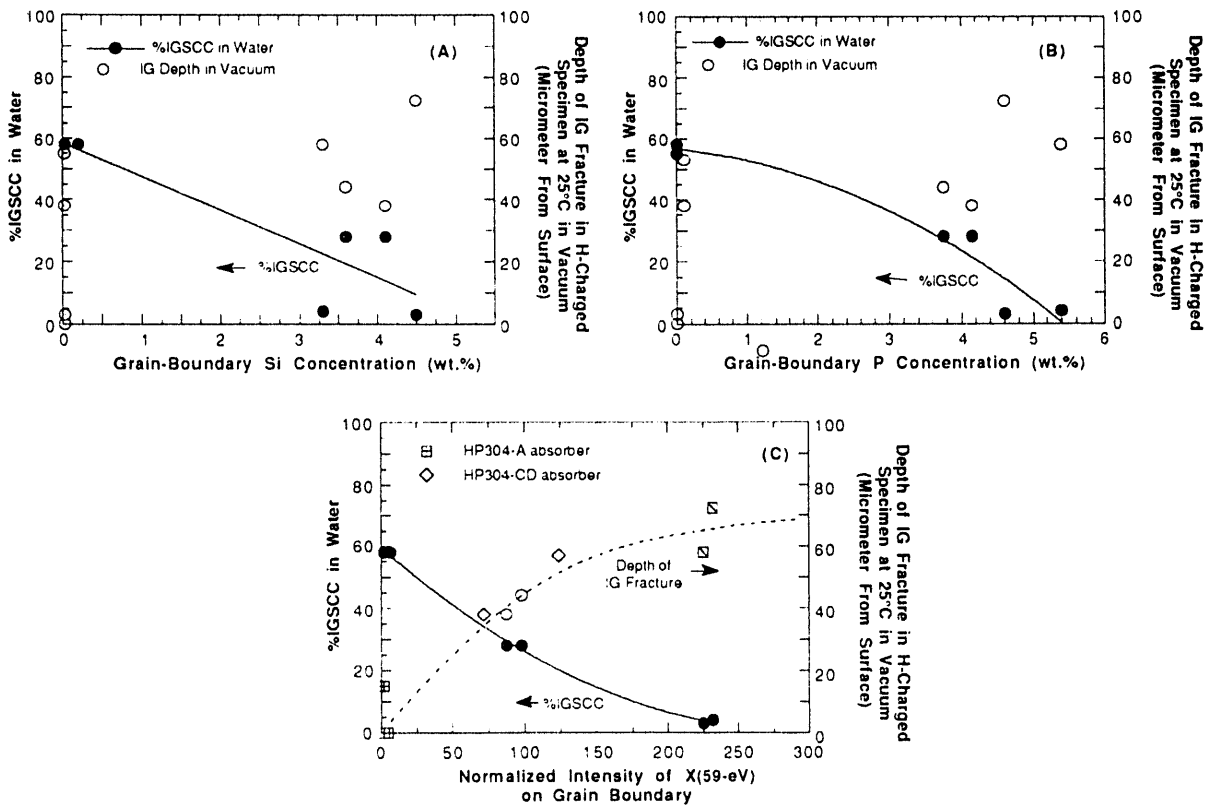

Fig. 5. Percent IGSCC in water and depth of intergranular fracture penetration in hydrogen-charged specimens, fractured at 25°C in vacuo, as a function of grain-boundary segregation of Si (A), P (B), and X (59-eV) (C). Fluence level of the specimens was ≈2 x 10^{21} n/cm^2.

function of the grain-boundary concentration of Si and P. Data for the grain-boundary segregation of Si, P, and other impurities has been reported in Refs. 12 and 13. In Figs. 5A-5C, the depth of IG-fracture penetration, produced in H-charged specimens in vacuo at 25°C, has also been plotted. The X(59-eV) peak shown in Fig. 5C is produced by the secondary Auger electrons of Li and Ni. A more detailed analysis to identify the origin of the peak is given later in this paper. No evidence of segregation of S was observed.[13]

No good correlation was observed between the susceptibility to H-enhanced IG cracking and grain-boundary concentration of Si or P. The percent IGSCC in water decreased monotonically for increased grain-boundary concentrations of Si, P, and X(59-eV). It is difficult, therefore, to explain the significant IGSCC in the HP absorber tube specimens or the negligible SCC susceptibility of the CP sheath specimens on the basis of grain-boundary segregation of Si, P, or S. The present results show convincingly that grain boundary segregation of Si, P, or S is not the mechanism of IASCC of Type 304 SS as has been speculated previously. Furthermore, the results also imply that the low content of Si, P, or S is not the primary factor associated with the better resistance of HP Type 348 SS.[6-9]

Effect of Cr Depletion

Minimum Cr on grain boundaries of the CP and HP absorber tubes and control blade sheath was determined by an AES depth-profile technique[12,13] and was correlated with percent IGSCC in Fig. 6. In the figure, similar results from FEG-STEM[9,20,21] are also plotted for comparison. The latter results were obtained on CERT specimens tested in simulated BWR water containing 8-32 ppm of dissolved O. For a better comparison, percent IGSCC from the present CERT tests conducted with ≈0.3 ppm dissolved O was extrapolated to an O content of 8-32 ppm according to the trend reported by Kodama et al.[19] A comparison similar to that of Fig. 6 has been discussed by Bruemmer et al.[22]

Results obtained by the two techniques appear to be consistent except for HP304-A, in which the Cr depletion profile was extremely narrow and deep according to AES. A more direct comparison of the AES and FEG-STEM data has been given elsewhere.[13] Fig. 6 could be interpreted as suggesting that the FEG-STEM data referred to in Fig. 6 have significant limitations when used to detect Cr content <14 wt.% within ≈1.5 nm of a grain boundary in BWR-irradiated specimens.

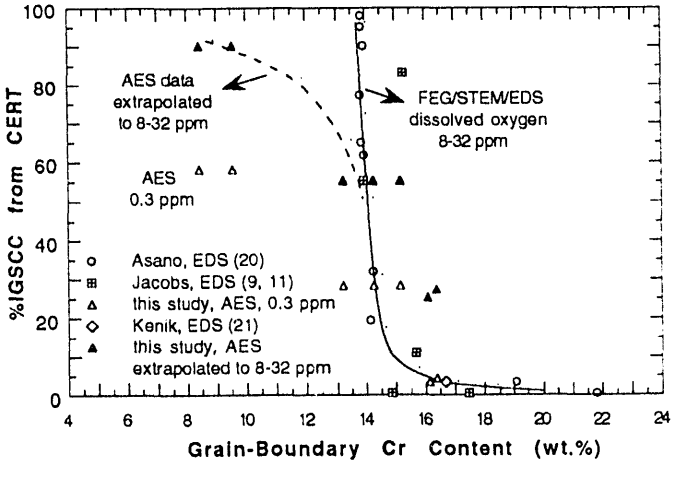

Fig. 6. Percent IGSCC vs. minimum grain-boundary Cr content determined from CERT tests and AES and FEG-STEM analyses of BWR components.

This may be because several limitations are inevitably associated with energy-dispersive spectroscopy (EDS) in the present-generation FEG-STEM. These limitations are the effects of imperfect grain-boundary alignment (e.g., 1-nm uncertainty produced with 1° misalignment in 57-nm-thick film), relatively large beam size, beam broadening,[23,24] effect of a Cr_2O_3 surface layer, and fluoresced Cr X-ray.[9] Because of these limitations, practical resolution in the present-generation FEG-STEM-EDS analysis should be considered close to 3-3.5 nm. This seems to be inadequate to analyze specimens from BWR components in which the Cr-depletion profile is very narrow. The resolution limit can be greatly improved by utilizing the technique of electron energy loss spectroscopy (EELS).[24] Meanwhile, AES data can suffer from the effect of O contamination from the vacuum environment of the microscope.

Without a proper understanding of the limitations of the techniques and uncertainties of measurement, and in the absence of a more convincing database (e.g., data from EELS with a more powerful FEG-STEM), the role of grain-boundary Cr depletion in IASCC (i.e., primary or secondary role) cannot be convincingly determined at the present time. Figure 6, however, indicates that susceptibility is increased significantly by Cr depletion, in particular for percent IGSCC<30% (i.e., lower fluence level). Nevertheless, the large variation in percent IGSCC for a similar grain-boundary Cr content of ≈14-15 wt.% (FEG-STEM data) appears to suggest that an unidentified process other than Cr depletion plays an important role.

Comparative Analysis of Two Similar High-Purity Heats

To provide a clue to the question of whether one or more unidentified processes play an important role in IASCC, a study was conducted with absorber tube specimens that were fabricated from the two virtually identical HP heats, HP304-A (less resistant to IGSCC during CERT tests)[12,17] and HP304-CD (more-resistant to IGSCC during CERT tests[17] and resistant to IASCC failure in reactor[11]). The specimens were irradiated to a similar fluence level of $\approx 2.0 \times 10^{21}$ n/cm^2. The rationale was that because Si, P, S, C, Ni, Cr, Mn and fluence levels were virtually the same in the two heats, grain-boundary concentrations of these elements and irradiation-induced hardening would also be similar. Therefore, it would be relatively easy to identify other aspects of grain-boundary chemistry, which could be correlated with resistance to IGSCC. The two materials also exhibited a surprisingly large difference in their susceptibility to hydrogen-induced IG fracture in vacuo (see Fig. 5C). In contrast to HP304-CD, it was very difficult to produce IG fracture in vacuum in H-charged specimens of HP304-A, a trend opposite to the susceptibility to IGSCC in water.

Grain-boundary Cr depletion in the two specimens, determined by the AES depth-profiling, is shown in Fig. 7. Not surprisingly, Cr depletion in the specimens was similar.

Grain-boundary segregation behavior of Ni and impurities in the two materials is shown in Fig. 8, where the segregation behavior of Ni, Si, P, C, S, N, X(59-eV), and B can be determined by comparing intensities of the elements on ductile (denoted "D") and intergranular (denoted "I") fracture surfaces. The left- and right-hand columns of Fig. 8 show results measured on HP304-A and HP304-CD, respectively. In Fig. 9, duplicate results obtained from another specimen of HP304-CD are given. In the HP304-A specimen, only Ni segregation was evident. In the HP304-CD specimen, grain-boundary segregation of not only Ni but also of N, X(59-eV), and B was evident. Figures 8H and 9D indicate some extent of segregation of C in the specimens of HP304-CD, although the evidence should be considered less convincing.

Identification of Li on Grain Boundaries

To identify the X(59-eV) peak, Auger spectra were obtained from several types of SS specimens, i.e., irradiated, unirradiated, and Li-corroded specimens. The results are summarized in Fig. 10. The X(59-eV) peak was observed in Auger spectra obtained from irradiated Type 304 SS BWR components (Fig. 10D), unirradiated Type 304 SS specimens

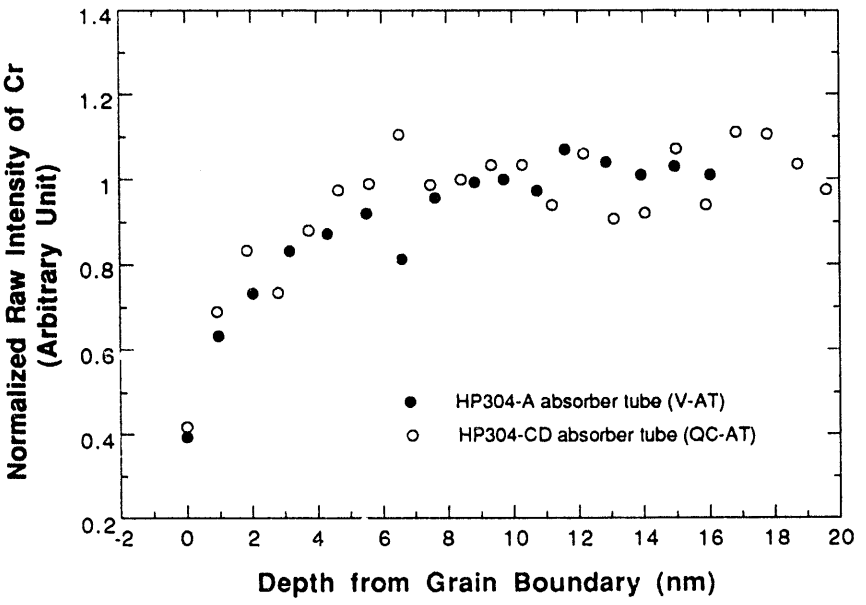

Fig. 7. Grain-boundary Cr-depletion profiles determined by AES analyses of HP304-A and HP304-CD absorber tubes irradiated to 2 x 10^{21} n/cm^2.

that were corroded in liquid Li (at 600°C for 144 h) (Fig. 10B), unirradiated 20 wt.%-Ni Type 310 SS (Fig. 10C), and unirradiated 35 wt.%-Ni Type 330 SS. The characteristic shape of the peak observed in the unirradiated high-Ni 310 SS was somewhat different from those observed in the Li-corroded or irradiated 304 SS specimens. The peak was absent in unirradiated specimens of Types 304, 347, AISI 3340, and martensitic SS, as shown in Fig. 11.

Results from these experiments show that at least some fraction of the intensity of the X(59-eV) peak observed in the specimens of HP304-CD (Figs. 8O and 9G) is due to Li. However, results in Figs. 8A, 8E, and 9A show that the segregation ratios of Ni in HP304-A and HP304-CD are virtually identical. Therefore, grain-boundary concentrations of Ni in the two specimens should be similar, because the bulk concentration of Ni is virtually the same (i.e., 9.45 wt.%; see Table 1). Accordingly, it is difficult to attribute the large difference in the intensities of the X(59-eV) peak between HP304-A (Fig. 8K) and HP304-CD (Fig. 8O) to grain-boundary concentrations of Ni. Segregation behaviors of X(59-eV) (Figs. 8O and 9G) and B (Figs. 8P and 9H) in HP304-CD were also similar. Therefore, we conclude that the X(59-eV) peak observed on the grain boundaries of HP304-CD is, in fact, the secondary peak (≈58 eV) of Li, whereas the primary peak of Li (≈43 eV) was superimposed on the 47-eV peak of Fe.

Li is produced by transmutation of ^{10}B dissolved in specimens by thermal neutrons, i.e., ^{10}B(n, He)^{7}Li. The cross section for this reaction is large, i.e., ≈3840 barn. Natural B dissolved in the absorber tubes is composed of 19.8% ^{10}B and 80.2% ^{11}B. However, it is not clear if one can rule out the possibility that some of the Li atoms detected in the absorber tubes were transported from the side of the B_4C absorber that is enriched in ^{10}B.

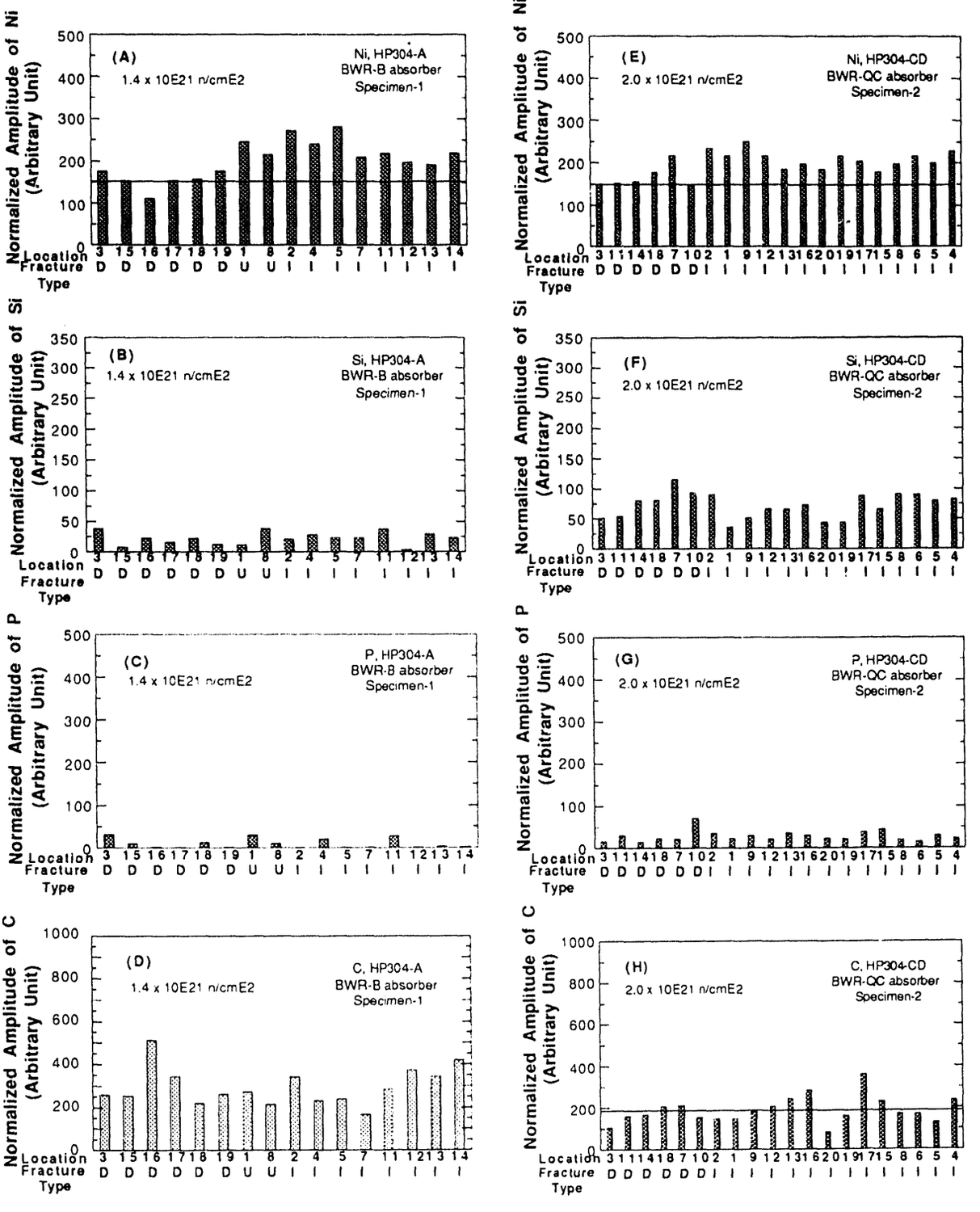

Fig. 8. Intensities of Ni, Si, P, C, S, N, X(59-eV), and B signals from ductile (Denoted by "D"), intergranular ("I"), and faceted ("U") fracture surfaces of the neutron absorber tubes fabricated from HP Heats HP304-A (left columns) and HP304-CD (right columns) and irradiated to ≈2.0 x 10^{21} n/cm^2. When grain-boundary segregation of an element is clear, a horizontal line was drawn to show average intensity of the element away from grain boundaries.

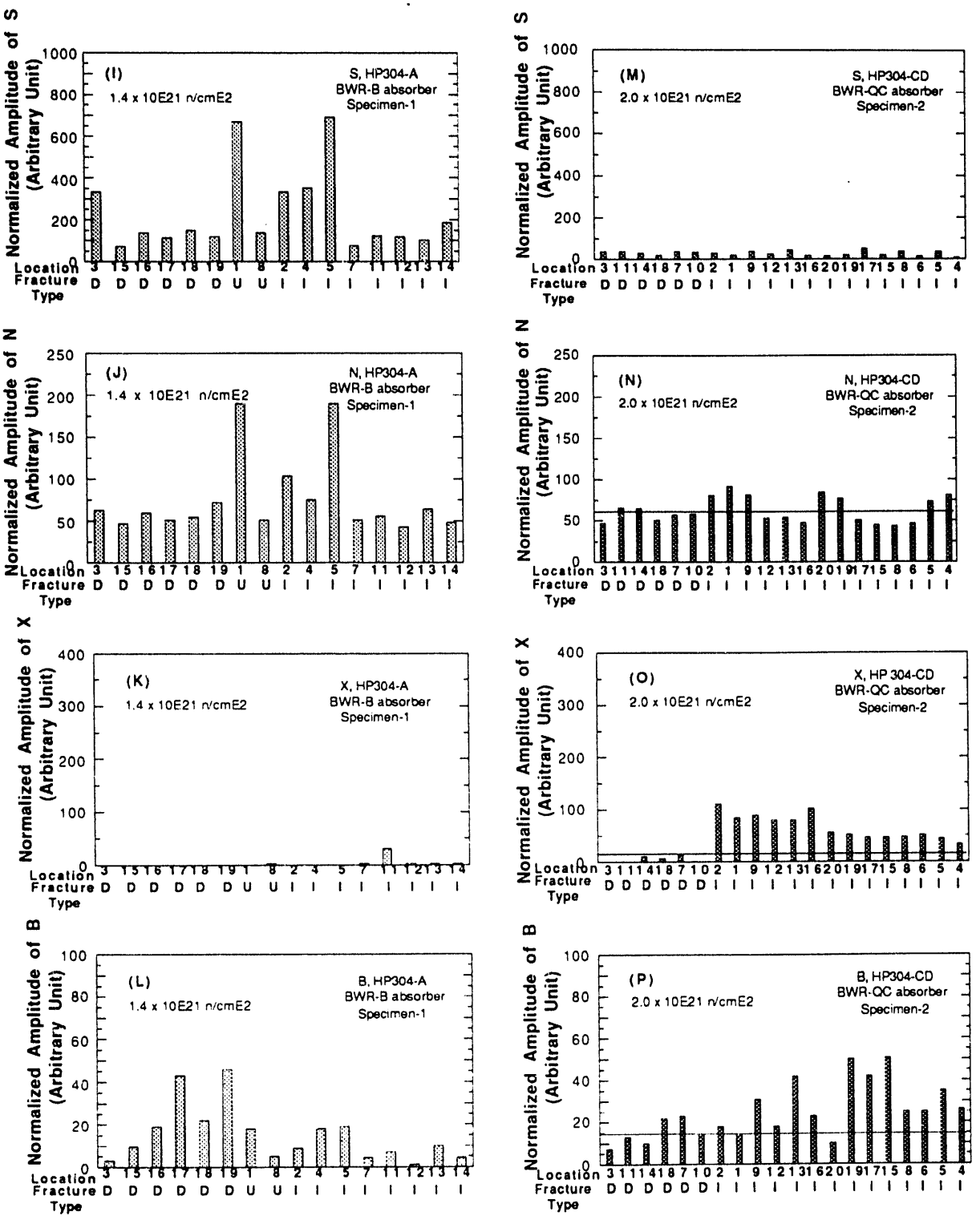
(I)
1.4 x 10E21 n/cmE2
S, HP304-A
BWR-B absorber
Specimen-1
(M)
2.0 x 10E21 n/cmE2
S, HP304-CD
BWR-QC absorber
Specimen-2
(J)
1.4 x 10E21 n/cmE2
N, HP304-A
BWR-B absorber
Specimen-1
(N)
2.0 x 10E21 n/cmE2
N, HP304-CD
BWR-QC absorber
Specimen-2
(K)
1.4 x 10E21 n/cmE2
X, HP304-A
BWR-B absorber
Specimen-1
(O)
2.0 x 10E21 n/cmE2
X, HP 304-CD
BWR-QC absorber
Specimen-2
(L)
1.4 x 10E21 n/cmE2
B, HP304-A
BWR-B absorber
Specimen-1
(P)
2.0 x 10E21 n/cmE2
B, HP304-CD
BWR-QC absorber
Specimen-2
Normalized Amplitude of S (Arbitrary Unit)
Normalized Amplitude of N (Arbitrary Unit)
Normalized Amplitude of X (Arbitrary Unit)
Normalized Amplitude of B (Arbitrary Unit)
Location
Fracture Type

Fig. 8. Cont.

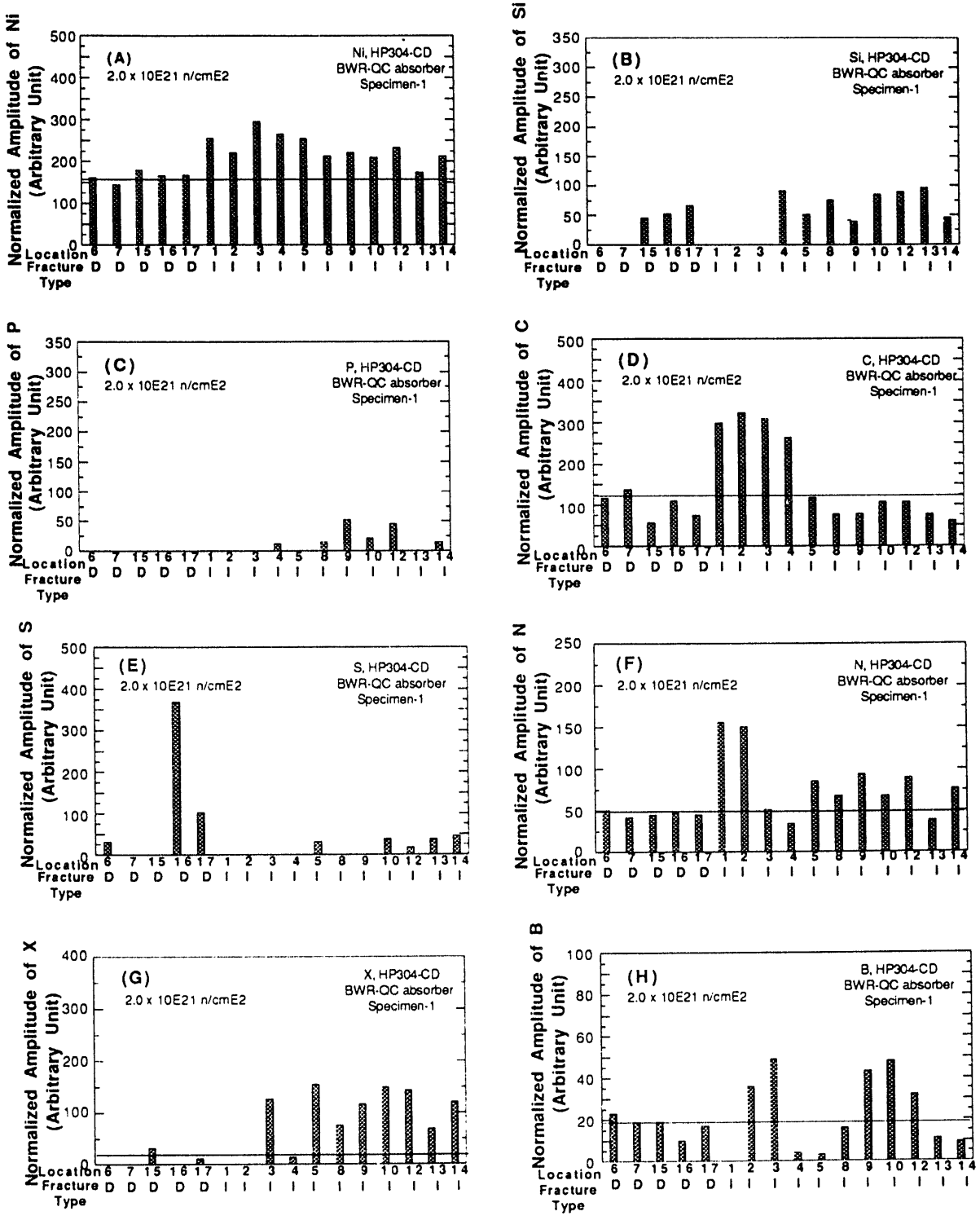

Fig. 9. Intensities of Ni, Si, P, C, S, N, X (59-eV), and B signals (A to H) from ductile (denoted by "D"), intergranular ("I"), and faceted ("U") fracture surfaces of a duplicate specimen from neutron absorber tubes fabricated from HP Heat HP304-CD irradiated to ≈2.0 x 10^{21} n/cm. When grain-boundary segregation of an element is clear, a horizontal line was drawn to show average intensity of the element away from grain boundaries.

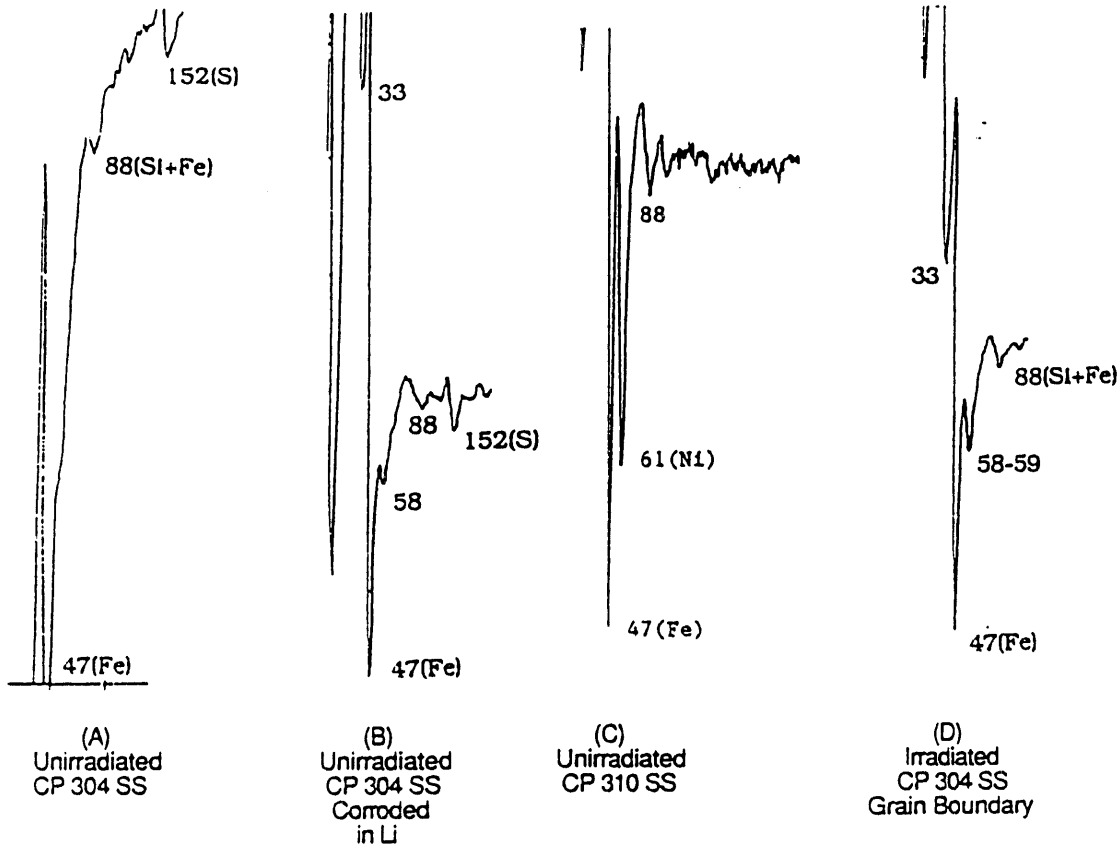

Fig. 10. Characteristic ≈59-eV Auger electron peaks obtained from (A) unirradiated CP Type 304; (B) Type 304 unirradiated and corroded in liquid lithium at 600°C for 144 h; (C) unirradiated Type 310 containing ≈20 wt.% Ni, and (D) CP Type 304 irradiated to 2 x 10^{21} n/cm^2.

In austenitic steels, B is known to segregate strongly to grain boundaries by a thermal process. Therefore, grain-boundary concentrations of B, and hence Li, could be influenced by the fabrication process in the absorber tubes, even if the tubes were extruded from the same starting material. In a slowly cooled section of a thick component (e.g., BWR top guide), thermal segregation of B is likely to be more pronounced. When segregated, ^{10}B was transmuted to Li and He in the absorber tubes, and Li was scattered away in the vicinity of grain boundaries because of recoil energy from the transmutation. Under these conditions, Li atoms in the HP304-CD specimens seem to have segregated to grain boundaries by the RIS process in significant quantity because the grain-boundary regions were relatively richer in Li. Lithium segregation in HP304-A was negligible, apparently because bulk concentration of B was lower and thermal segregation of B was insignificant during fabrication (Fig. 8L).

Effects of N, B, and Transmutation

Based on grain-boundary segregation behavior (Figs. 7-9) and bulk chemical composition (Table 1), grain-boundary concentrations of alloying and impurity elements in the HP304-A and HP304-CD specimens have been calculated and plotted in Fig. 12. The grain-boundary concentrations were normalized in the plot to facilitate easy comparison of the two materials, with actual numbers given for each element.

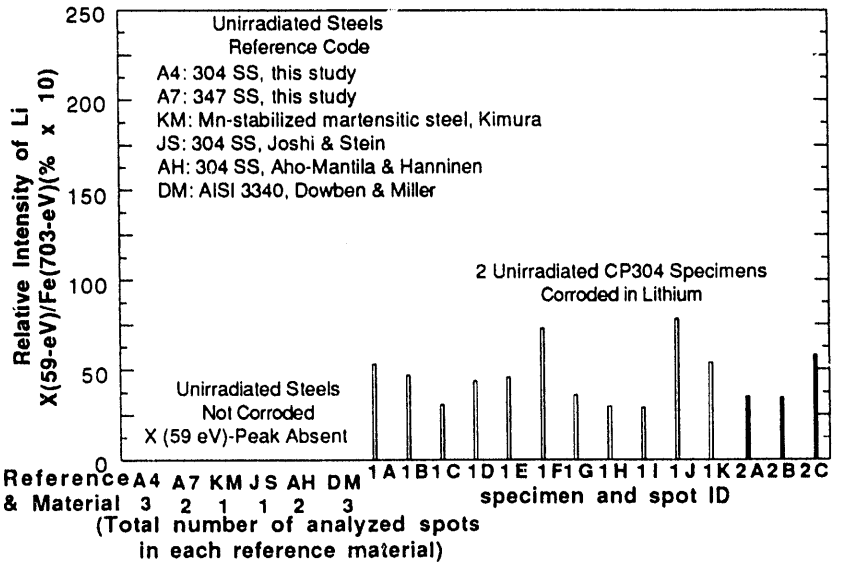

Fig. 11. Intensities of the ≈59-eV Auger electron peaks obtained from several types of unirradiated steels either as-received or corroded in liquid Li at 600°C for 144 h.

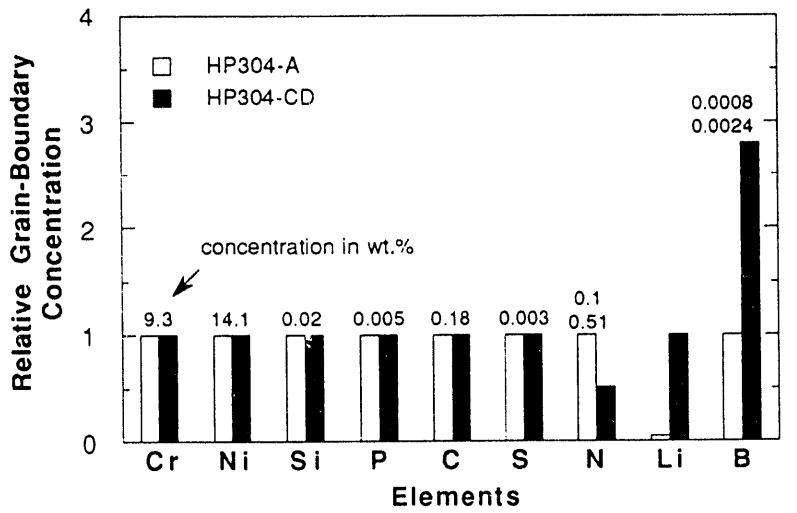

Fig. 12. Relative grain-boundary concentrations of alloying and impurity elements in HP304-A and HP304-CD absorber tube specimens irradiated to ≈2 x 10^{21} n/cm^2.

Figure. 12 shows that grain-boundary concentrations of the two materials are virtually the same, except for N, Li, and B. Grain-boundary concentrations of Cr, Ni, Si, P, C, and S are similar. Therefore, we conclude that higher concentrations of N and lower concentrations of Li and B on grain boundaries are conducive to higher susceptibility to IGSCC.

Higher contents of N and B are known to enhance grain-boundary cohesion in unirradiated steels.[25] However, results of the present investigation indicate an opposite role for N in irradiated steels. The exact mechanism whereby higher N on grain boundaries promotes IGSCC in irradiated materials is not clear. Segregation of N results in a higher concentration of H near grain boundaries because of transmutation of N to H (proton) by thermal neutrons, i.e., $^{14}N(n, p)^{14}C$. The cross section for this reaction is ≈1.83 barn. Although H atoms produced from the reaction recoil from grain boundaries, transmutation of segregated N nevertheless promotes an accumulation of H near a grain-boundary crack tip. The mechanism whereby a greater concentration of Li on grain boundaries is conducive to lower susceptibility to IGSCC is not clear either.

The present study strongly indicates that a synergism between grain-boundary segregation of impurities (N and B) and transmutation by thermal neutrons plays an important role in IASCC. It also suggests that the relative importance of the role of grain-boundary Cr depletion may be not as great as previously believed.

CONCLUSIONS

1. Resistance of in-core components fabricated from high-purity Type 304 stainless steel to irradiation-assisted stress corrosion cracking (IASCC) is not necessarily superior to that of fabricated from commercial-purity materials. Contrary to previous beliefs, susceptibility to intergranular stress corrosion cracking (IGSCC) could not be correlated with radiation-induced segregation (RIS) of Si, P, C, or S, but a correlation was obtained with grain-boundary Cr concentration, indicating that Cr depletion influences IASCC.

2. Grain-boundary concentrations of Cr determined by Auger electron spectroscopy (AES) and X-ray energy dispersive spectroscopy (EDS) in currently available field-emission-gun scanning transmission electron microscopes are not sufficiently accurate to clarify the importance of the role of irradiation-induced depletion of grain-boundary Cr (i.e., primary or secondary role). Irradiation-induced Cr depletion and thermal sensitization could conjointly increase susceptibility of weldments and heat affected zones of in-core components to IGSCC.

3. Grain-boundary analysis was conducted on BWR neutron absorber tubes that were fabricated from two HP heats of Type 304 SS of virtually identical chemical composition but differing significantly in susceptibility to IGSCC after irradiation to similar fluence levels. Grain-boundary concentrations of Cr, Ni, Si, P, S, and C of the crack-resistant and -susceptible tubes were virtually identical; however, grain boundaries of the cracking-resistant material contained lower concentrations of N and higher concentrations of B and Li than the crack-susceptible material.

4. Boron segregates strongly to grain boundaries by a thermal process in austenitic steels. Therefore, grain-boundary concentrations of B, and hence Li, could be influenced strongly by thermomechanical processes. Even if core-internal components are fabricated from the same starting material, actual grain-boundary concentrations of B and Li could differ significantly during service. In slowly cooled sections of a thicker component (e.g., BWR top guide), segregation of B, and hence Li, is likely to be more pronounced. This is conducive to better resistance to IASCC under otherwise similar conditions.

5. The present study indicates that a synergism between grain-boundary segregation (of impurities) and transmutation by neutrons plays an important role in IASCC.

ACKNOWLEDGMENTS

The authors are grateful to G. Dragel, D. Donahue, and G. J. Talaber for their experimental contributions. The BWR components were obtained through the kind assistance of Dr. A. J. Jacobs of General Electric Company. This work was sponsored by the

Office of Nuclear Regulatory Research, U.S. Nuclear Regulatory Commission. The authors are also grateful to Drs. J. Muscara and W. J. Shack for helpful discussions.

REFERENCES

1. J. Low, U. Wolff, and W. Cowden, "Electron Microscopic Examination of Failed Stainless Steel Fuel Cladding – Dresden Advanced Fuel Assemblies PF-1 and PR-4," APED-4242, General Electric Co., May 1963.
2. J. S. Armijo, "Effect of Impurity Additions on the Intergranular Corrosion of High Purity Fe-Cr-Ni Austenitic Alloys," GEAP-5047, General Electric Co., October 1966.
3. J. S. Armijo, "Grain Boundary Studies of Austenitic Stainless Steels," GEAP-5503, General Electric Co., September 1967.
4. J. S. Armijo, "Intergranular Corrosion of Nonsensitized Austenitic Stainless Steels," Corrosion 24 (1968), 24-30.
5. R. Duncan, "Stainless Steel Failure Investigation Program," GEAP-5530, General Electric Co., February 1968.
6. A. Strasser, J. Santucci, K. Lindquist, W. Yario, G. Stern, L. Goldstein, and L. Joseph, "Evaluation of Stainless Steel Cladding in LWRs," EPRI NP-2642, Electric Power Research Institute, Palo Alto, CA, December 1982.
7. F. Garzarolli, D. Alter, and P. Dewes, "Deformability of Austenitic Stainless Steels and Ni-Base Alloys in the Core of a Boiling and Pressurized Water Reactor," Proc. 2nd Int. Symp. Environmental Degradation of Materials in Nuclear Power Systems – Water Reactors, National Association of Corrosion Engineers, Houston, pp. 131–138 (1986).
8. F. Garzarolli, D. Alter, P. Dewes, and J. L. Nelson, "Deformability of Austenitic Stainless Steels and Ni-Base Alloys in the Core of a Boiling and Pressurized Water Reactor," Proc. 3rd Int. Symp. Environmental Degradation of Materials in Nuclear Power Systems – Water Reactors, G. J. Theus and J. R. Weeks, eds., The Metallurgical Society, Warrendale, PA, pp. 657–664 (1988).
9. A. J. Jacobs, R. E. Clausing, M. K. Miller, and C. Shepherd, "Influence of Grain Boundary Composition on the IASCC Susceptibility of Type 348 Stainless Steel," Proc. 4th Int. Symp. Environmental Degradation of Materials in Nuclear Power Systems – Water Reactors, National Association of Corrosion Engineers, Houston, pp. 14–21 to 14–45 (1990).
10. A. J. Jacobs, G. P. Wozadlo, K. Nakata, T. Yoshida, and I. Masaoka, "Radiation Effects on the Stress Corrosion and Other Selected Properties of Type-304 and Type-316 Stainless Steels," Proc. 3rd Int. Symp. Environmental Degradation of Materials in Nuclear Power Systems – Water Reactors, G. J. Theus and J. R. Weeks, eds., The Metallurgical Society, Warrendale, PA, pp. pp. 673–681 (1988).
11. A. J. Jacobs, "The Relationship of Grain Boundary Composition in Irradiated Type 304 SS to Neutron Fluence and IASCC," Effects of Radiation on Materials: 16th Intl. Symp., ASTM STP 1175, A. S. Kumar, D. S. Gelles, R. K. Nanstad, and T. A. Little, eds., American Society for Testing and Materials, Philadelphia (1993).
12. H. M. Chung, W. E. Ruther, J. E. Sanecki, A. G. Hins, and T. F. Kassner, "Stress Corrosion Cracking Susceptibility of Irradiated Type 304 Stainless Steels," Effects of Radiation on Materials: 16th Int. Symp., ASTM STP 1175, A. S. Kumar, D. S. Gelles, R. K. Nanstad, and T. A. Little, eds., American Society for Testing and Materials, Philadelphia (1993).
13. H. M. Chung, W. E. Ruther, J. E. Sanecki, and A. G. Hins, in Environmentally Assisted Cracking in Light Water Reactors: Semiannual Report April-September 1992, NUREG/CR-4667, Vol. 15, ANL-93/2, Argonne National Laboratory, pp. 28-60, June 1993.
14. K. Fukuya, S. Shima, H. Kayano, and M. Narui, "Stress Corrosion Cracking and Intergranular Corrosion of Neutron-Irradiated Austenitic Steels," J. Nucl. Mater., 191-194 (1992), 1007-1011.

15. K. Fukuya, K. Nakata, and A. Horie, "An IASCC Study Using High-Energy Ion Irradiation," Proc. 5th Int. Symp. Environmental Degradation of Materials in Nuclear Power Systems – Water Reactors, American Nuclear Society, La Grange Park, IL, pp. 814-820 (1992).

16. J. M. Cookson, R. D. Carter, D. L. Damcott, M. Atzmon, G. S. Was, and P. L. Andresen, "Stress Corrosion Cracking of High-Energy Proton-Irradiated Stainless Steels," ibid., pp. 806-813.

17. A. J. Jacobs, General Electric Co., San Jose, CA, private communication, 1993.

18. P. L. Andresen, F. P. Ford, S. M. Murphy, and J. M. Perks, "State of Knowledge of Radiation Effects on Environmental Cracking in Light Water Reactor Core Materials," Proc. 4th Int. Symp. Environmental Degradation of Materials in Nuclear Power Systems – Water Reactors, National Association of Corrosion Engineers, Houston, pp. 1-83 to 1-121 (1990).

19. M. Kodama, S. Nishimura, J. Morisawa, S. Shima, S. Suzuki, and M. Yamamoto, "Effects of Fluence and Dissolved Oxygen on IASCC in Austenitic Stainless Steels," Proc. 5th Int. Symp. Environmental Degradation of Materials in Nuclear Power Systems – Water Reactors, American Nuclear Society, La Grange Park, IL, pp. 948-954 (1992).

20. K. Asano, K. Fukuya, K. Nakata, and K. Kodama, "Changes in Grain Boundary Composition by Neutron Irradiation on Austenitic Stainless Steels," ibid. pp. 838-843.

21. E. A. Kenik, "Radiation-Induced Segregation in Irradiated Type 304 Stainless Steels," J. Nucl. Mater. 187 (1992), 239-246.

22. S. M. Bruemmer, B. W. Arey, and L. A. Charlot, "Influence of Chromium Depletion on the Intergranular Stress Corrosion Cracking of 304 Stainless Steel," Corrosion 48 (1992), 42-49.

23. D. I. R. Norris, C. Baker, and J. M. Titchmarsh, "Compositional Profiles at Grain Boundaries in 20%Cr/25%Ni/Nb Stainless Steel," Proc. Symp. on Radiation-Induced Sensitization of Stainless Steels, D. Norris ed., Central Electricity Generating Board, Berkeley, England, pp. 86-98, 1987.

24. J. M. Titchmarsh and I. A. Vatter, "Measurement of Radiation-Induced Segregation Profiles by High Spatial Resolution Electron Microscopy," ibid., pp. 74-85.

25. M. Polak, "Interfacial Segregation in Steel and Steels-Related Alloys," in Surface Segregation Phenomena, P. A. Dowben and A. Miller eds., CRC Press, Boca Raton, FL, pp. 291-325, 1990.

END

DATE
FILMED
3/28/94